



Citation for published version:

Manning, H, Chong, TH, Carr, D & Bird, MR 2016, 'Critical flux of Gum Arabic: implications for fouling and fractionation performance of membranes', *Food and Bioproducts Processing*, vol. 97, pp. 41-47.
<https://doi.org/10.1016/j.fbp.2015.10.005>

DOI:

[10.1016/j.fbp.2015.10.005](https://doi.org/10.1016/j.fbp.2015.10.005)

Publication date:

2016

Document Version

Peer reviewed version

[Link to publication](#)

University of Bath

General rights

Copyright and moral rights for the publications made accessible in the public portal are retained by the authors and/or other copyright owners and it is a condition of accessing publications that users recognise and abide by the legal requirements associated with these rights.

Take down policy

If you believe that this document breaches copyright please contact us providing details, and we will remove access to the work immediately and investigate your claim.

CRITICAL FLUX OF GUM ARABIC: IMPLICATIONS FOR FOULING AND FRACTIONATION PERFORMANCE OF MEMBRANES

Harriet E. Manning^{1,2}, Tzyy Haur Chong^{3,4}, David Carr⁵, Michael R. Bird^{2*}

¹Centre for Sustainable Chemical Technologies, University of Bath, BA2 7AY, UK

²Membrane Applications Laboratory, Department of Chemical Engineering, University of Bath, BA2 7AY, UK

³School of Civil and Environmental Engineering, Nanyang Technological University, Singapore

⁴Singapore Membrane Technology Center, Nanyang Environment and Water Research Institute, Nanyang Technological University, Singapore

⁵Kerry Ingredients & Flavours, Draycott Mills, Cam, Dursley, Gloucestershire, GL11 5NA, UK

*Corresponding author. E-mail address: M.R.Bird@bath.ac.uk

ABSTRACT

A flux-stepping method was used to determine the critical flux of 2 wt% gum arabic using flat sheet polysulfone membranes. These were found to be 27 L m⁻² h⁻¹, 10 L m⁻² h⁻¹ and 22 L m⁻² h⁻¹ for 0.1, 0.5 and 0.8 μm polysulfone membranes, respectively. Increasing the cross flow velocity was found to raise the critical flux, although the effect diminished at higher velocities. These values were then used to assess the fouling and the fractionation performance of the three membranes above and below their critical fluxes.

Keywords: Microfiltration, gum arabic, critical flux, fouling, membrane fractionation, flux-stepping

1. INTRODUCTION

The fractionation of gum arabic into its three component parts has long been considered a desirable aim industrially. Gum arabic processing is a 50,000 tonnes per year industry and the processed product is widely used in the food industry as an emulsifying, stabilising, thickening and glazing agent. It has been shown that *Acacia senegal* contains between 10 and 20 wt% arabinogalactan – protein complex (AGP; Average MW = 1500 kDa), which is the functional component giving gum arabic its exceptional properties as an emulsifying agent (Nishino *et al.*, 2012; Randall *et al.*, 1988). The other two fractions in gum arabic are arabinogalactan (AG; very broad MW range, average = 280 kDa; 75 - 90% total gum solids) and glycoprotein (GP; Average MW = 250 kDa; about 2% total gum solids). The aim of a number of studies has been to modify gum arabic to improve its properties as an emulsifier (Al-Assaf *et al.*, 2007; Fang *et al.*, 2013, Heidebach *et al.*, Katayama *et al.*, 2012, Ward, 2002). Another reason for the industrial interest in gum arabic fractionation is its potential to reduce batch-to-batch variation by separating the AGP and then blending it with other gum constituents in order to regulate the AGP content.

Previous work in our group has reported the first use of synthetic, polymeric membranes to separate the AGP fraction of gum arabic from the other two fractions present (arabinogalactan (AG) and glycoprotein (GP)) in cross-flow diafiltrations (Manning and Bird, 2015). Here, commercial polysulfone (PS) membranes of 0.1, 0.5 and 0.8 μm pore size were

tested for their fractionation performance. It was concluded that the smaller pore size membrane rejected the AGP to a greater extent, but that after some fouling of the membrane, the larger pore size membrane also showed some rejection. It was also observed that very little gum arabic passed through the 0.1 μm membrane, suggesting that the pore size was too small for the majority of the gum species to be transmitted. The fouling observed was, therefore, likely to be surface cake formation. Contrastingly, the larger pore sized membranes showed greater transmission of gum arabic initially, but this decreased over time. It seems likely that an initial pore blocking mechanism is subsequently followed by cake formation.

Field *et al.* (1995) first introduced the concept of critical flux. This phenomenon describes filtration upon start up that, below a threshold flux, demonstrates little or no membrane fouling. During filtrations at constant flux, this results in a steady trans-membrane pressure (TMP). If the flux is increased, however, above this critical value, fouling occurs which cannot be removed upon once again lowering the flux. When a membrane is fouled, the TMP increases under conditions of constant flux operation. This critical flux value can be improved by increasing the cross-flow velocity.

There exist two forms of this theory. The first is the ‘strong form’ of the critical flux, where a flux exists which is equal to the pure water flux under those conditions; the second is the ‘weak form’ where upon start up, a constant flux is quickly established, after some initial solute adsorption occurs, and continues with no rise in TMP.

Fouling can significantly alter the selectivity of the membrane; operating below critical flux has the advantage of easier control over the filtration conditions. This is interesting from the point of view of fractionation, as the absence of surface deposits may have an effect on the rejection of species. These deposits alter the filtration properties throughout the entire operation as the surface deposits will change in thickness and density, and in-pore blocking will also affect the pore size distribution, giving constantly changing results (Brans *et al.* (2004)).

This paper reports the determination of the critical flux of 2 wt% gum arabic using 0.1, 0.5 and 0.8 μm PS membranes and observes the effect on filtration and fractionation performance operating above and below the critical flux. The effect of CFV upon critical flux is also reported.

2. MATERIALS AND METHODS

2.1. Materials

Gum arabic was supplied by *Kerry Ingredients and Flavours* (Cam, Gloucestershire, UK) as a milled, raw product from *Acacia Senegal* trees in Sudan. Feed solutions were prepared by dissolving the appropriate amount of gum arabic in Milli-Q water and passing this through a 50 μm wound stainless steel pre-filter to remove insoluble debris. A concentration of 2 wt% was chosen for this work to provide a low viscosity feed and to be consistent with previous

work (Manning and Bird, 2015). Milli-Q water (Millipore) was used for feed preparation and filtrations.

Polysulfone (PS) membranes of 0.1, 0.5 and 0.8 μm pore size (MFG1, GRM-RT5 and GRM-RT8; *Alfa Laval*, Denmark) were cut to fit a crossflow filtration cell (Ying Kwang Trading, custom made). The cell has parallel plate geometry with an active membrane area of 0.0054 m^2 (0.18 m x 0.03 m) and a channel height of 1.5 mm. The set-up consisted of a 10 L feed tank fitted with an overhead stirrer (Panasonic, model MX8G5B) connected to a gear pump (Cole-Palmer, model 74013-45). Feed temperature was maintained at 40 $^{\circ}\text{C}$ by a heating/cooling system (Polyscience, model 9112) and permeate flux was controlled by a mass flow controller (Brooks Instrument, model 5882).

The membranes were conditioned before use to remove the glycerine coating by passing water at 60 $^{\circ}\text{C}$ over the membrane in the cross-flow cell utilizing the protocol developed by Weis *et al.* (2005).

2.2. Experimental procedure

The flux stepping method (Chen *et al.*, 1997) was used to determine the critical flux of 2 wt% gum arabic using 0.1, 0.5 and 0.8 μm PS membranes. New, conditioned membranes were used for each experiment. First, the TMP readings were recorded every 20 s for Milli-Q water over a range of fluxes. The operating conditions for this membrane pure water permeability were the same as for the fouling experiment of 2 wt% gum arabic. Standard filtration conditions were set at 40 $^{\circ}\text{C}$, a cross flow velocity (CFV) of 0.37 m s^{-1} , and 15 minute flux steps were carried out from 2 $\text{L m}^{-2} \text{h}^{-1}$ (LMH) until a flux where TMP increase over the step period was significant ($>0.02 \text{ bar min}^{-1}$), which indicates serious membrane fouling. For the 0.8 μm membranes, the flux stepping started at 10 LMH. Permeate and retentate were cycled back to the feed tank to maintain constant feed volume and concentration.

The effect of altering CFV was investigated by carrying out flux stepping experiments using 0.1 μm PS membranes at varying crossflow velocities (0.18, 0.37, 0.56 and 0.67 m s^{-1}). A total of 3 repeats of the critical flux measurement of 2 wt% gum arabic with 0.1 μm PS membranes at 0.37 m s^{-1} CFV were carried out to test the reproducibility of the experiments.

After determination of the critical flux of 2 wt% gum arabic with the 3 membrane pore sizes under standard conditions, longer diafiltration experiments were carried out both above and below the critical flux in order to study the effect of fouling on the filtration and fractionation performance of the membrane.

2.3. Data analysis

The critical flux of 2 wt% gum arabic at 40 $^{\circ}\text{C}$ and 0.37 m s^{-1} CFV was determined using the flux stepping method. There are several approaches for estimating the critical flux in this flux stepping method and two of these methods were employed here. Figure 1, modified from Le Clech *et al.* (2003), explains the two different parameters based on TMP used to identify the point at which membrane fouling occurred. The first parameter is the change in

TMP over the step period (15 minutes). This can be observed visually from the graphs of TMP vs. time. The critical flux is defined as the flux above which $dTMP / dt \neq 0$. This is also calculated using equation 1.

$$\frac{dTMP}{dt} = \frac{(TMP_{final} - TMP_{initial})}{(t_{final} - t_{initial})} \quad (1)$$

$TMP_{initial}$ is the average TMP over the first minute of the flux step, excluding the first data point and TMP_{final} is the average TMP over the last minute of the flux step. Time is represented by t .

A second parameter, the average TMP in each step (TMP_{av}) can be plotted against flux and the point at which the two are no longer proportional, or the point at which the permeability (K ; $L\ m^{-2}\ h^{-1}\ bar^{-1}$) is no longer linear, is defined as the critical flux. These two approaches give different information about the fouling of the membrane.

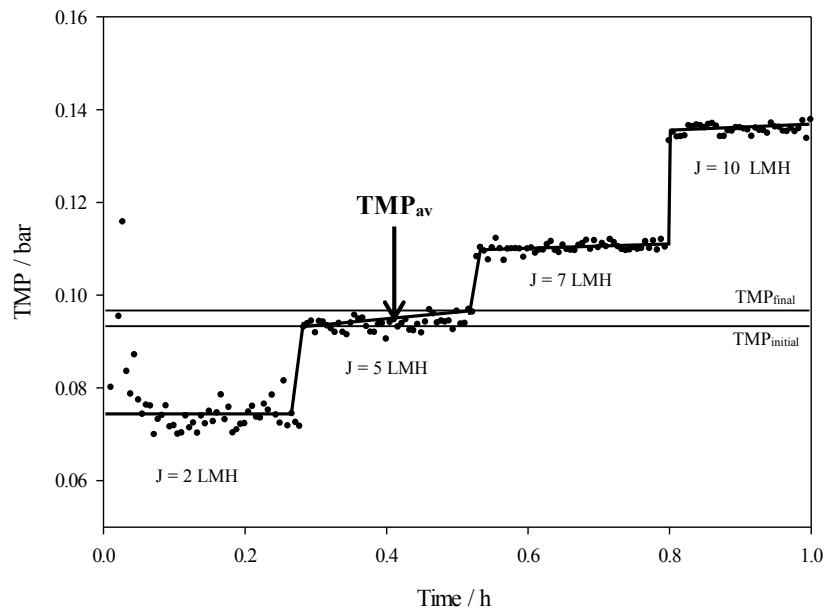


Figure 1: Explanation of the different parameters used to determine critical flux using the flux-stepping method. Modified from Le Clech *et al.* (2003).

3. RESULTS

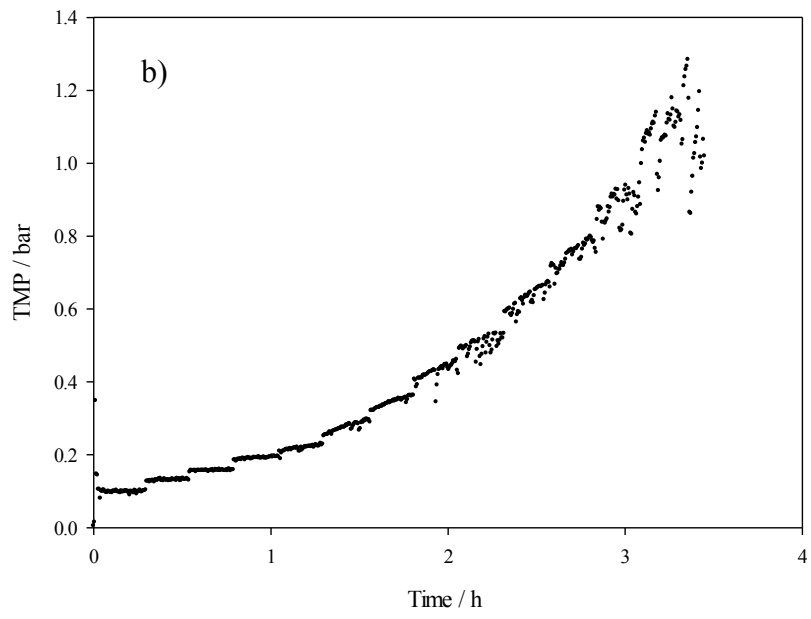
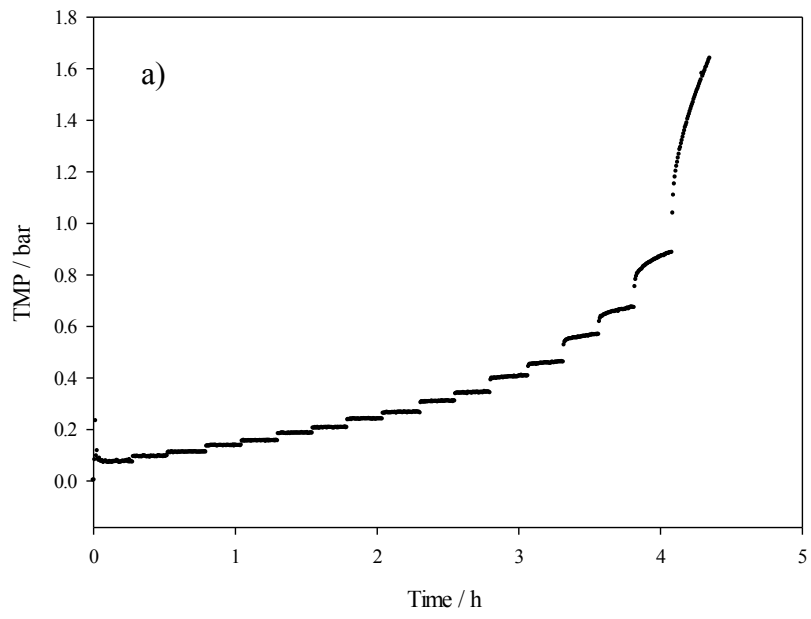
3.1. Pure water filtration

The membrane resistances were calculated from pure water flux measurements to be 1.05×10^{12} , 4.96×10^{11} and $2.48 \times 10^{11}\ m^{-1}$ for 0.1, 0.5 and 0.8 μm PS membranes, respectively.

3.2. Effect of membrane pore size

Figure 2 shows the TMP profile of the flux stepping for the filtration of 2 wt% gum arabic using 0.1, 0.5 and 0.8 μm PS membrane at 40 °C and a CFV of $0.37\ m\ s^{-1}$. The step intervals

were 15 minutes and the step size is indicated in the figure caption for each graph. The experiment was repeated 3 times using new 0.1 μm PS membranes each time and data shown for this membrane represent the mean values with error bars showing \pm one standard deviation.



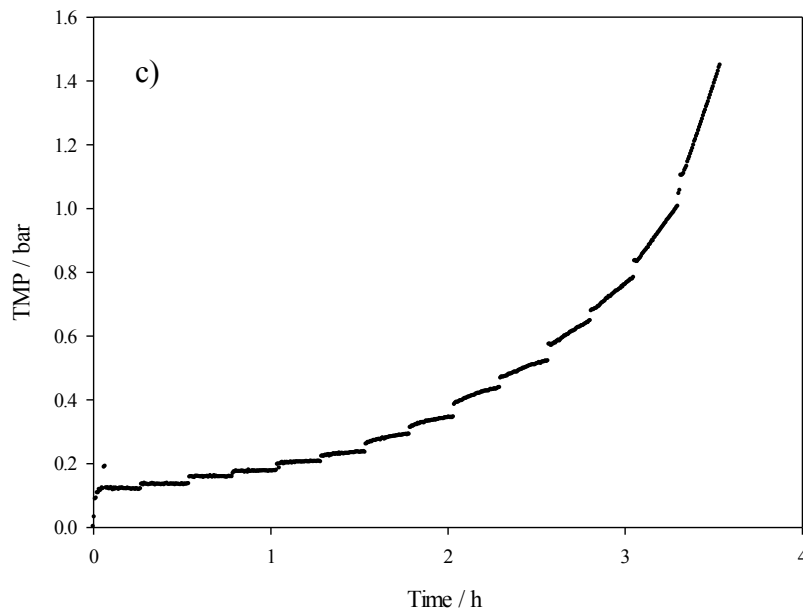


Figure 2: Flux steps of 15 minute duration of 2 wt% gum arabic filtration using a 0.1 μm PS (a) 0.5 μm PS (b) and 0.8 μm PS (c) membrane at 40 $^{\circ}\text{C}$, 0.37 m s^{-1} CFV. The steps are 2, 5, 7, 10, 12, 15, 17, 20, 22, 25, 27, 30, 32, 35, 37, 40 and 45 LMH (a), 2, 5, 7, 10, 12, 15, 17, 20, 22, 25, 27, 30 and 35 LMH (b) and 10, 12, 15, 17, 20, 22, 25, 27, 30, 32, 35, 37, 40 and 45 LMH (c).

The weak form of the critical flux can be estimated visually as the point at which the TMP no longer remains constant during the 15 minute flux step. These appear to be approximately 27 LMH, 10 LMH and 15 LMH for the 0.1, 0.5 and 0.8 μm membranes, respectively. The fouling rate is represented graphically in Figure 3 as a plot of $d\text{TMP}/dt$ vs flux. Figure 4 shows the average TMP as a function of flux. Critical fluxes can be determined as 27, 10 and 22 LMH for 0.1, 0.5 and 0.8 μm PS membranes, respectively.

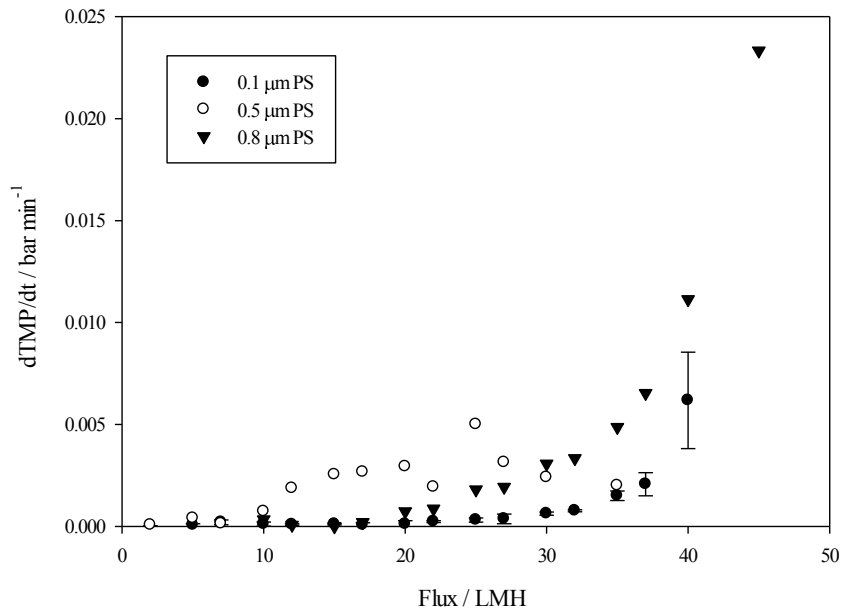


Figure 3: Fouling rate for 2 wt% gum arabic using 0.1, 0.5 and 0.8 μm PS membranes. The filtration temperature was 40 $^{\circ}\text{C}$ and the CFV was 0.37 m s^{-1}

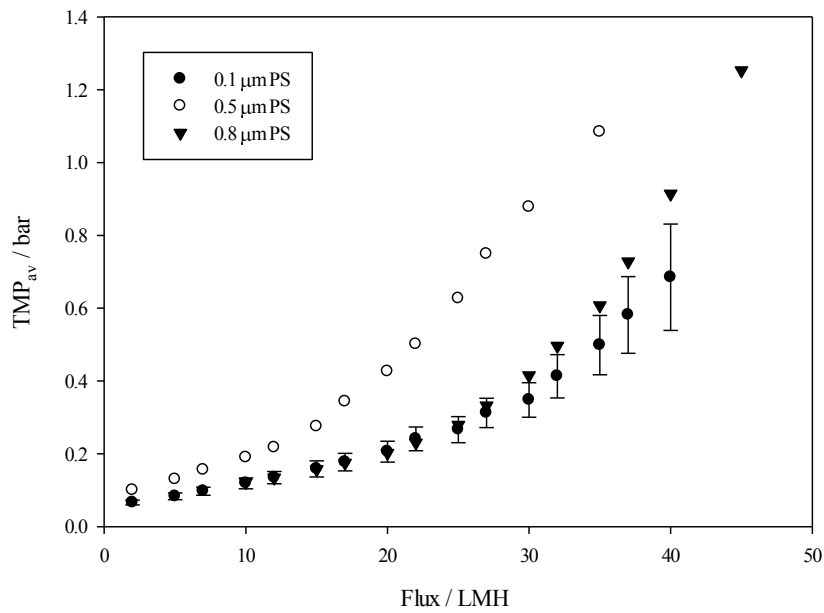


Figure 4: TMP_{av} for the filtration of 2wt% gum arabic with 0.1, 0.5 and 0.8 μm PS membranes as a function of flux. The temperature was 40 $^{\circ}\text{C}$ and CFV 0.37 m s^{-1}

The critical flux can also be defined as maximum flux at which the permeability (K) remains linear (Ye *et al.*, 2005). From Figure 4, these critical flux values are determined as 25, 12 and 22 LMH for 0.1, 0.5 and 0.8 μm membranes, respectively.

$$K = \frac{J}{\text{TMP}_{\text{av}}} \quad (2)$$

From Figure 4, K can be calculated as 113.6, 85.5, and 93.5 L m⁻² h⁻¹ bar⁻¹ for 0.1, 0.5 and 0.8 μm membranes, respectively. These values are all lower than the corresponding K values for pure water (625, 1667 and 3333 L m⁻² h⁻¹ bar⁻¹) which shows that the weak form of the critical flux is observed.

The total resistance for each membrane can be calculated using the following equation:

$$R_{\text{total}} = \frac{1}{\mu K} \quad (3)$$

where μ is the permeate viscosity. The R_{total} for 0.1, 0.5 and 0.8 μm membranes calculated from the K values above are 3.83 x 10¹², 4.75 x 10¹² and 3.08 x 10¹² m⁻¹, respectively, which again are all higher than the corresponding membrane resistances (1.05 x 10¹², 4.96 x 10¹¹ and 2.48 x 10¹¹ m⁻¹), demonstrating the presence of some initial fouling or adsorption on the membrane.

3.3. Effect of CFV

The effect of CFV on the critical flux was measured by carrying out flux stepping of 2 wt% gum arabic with 0.1 μm PS membranes at 0.18, 0.37, 0.56 and 0.67 m s⁻¹ CFV.

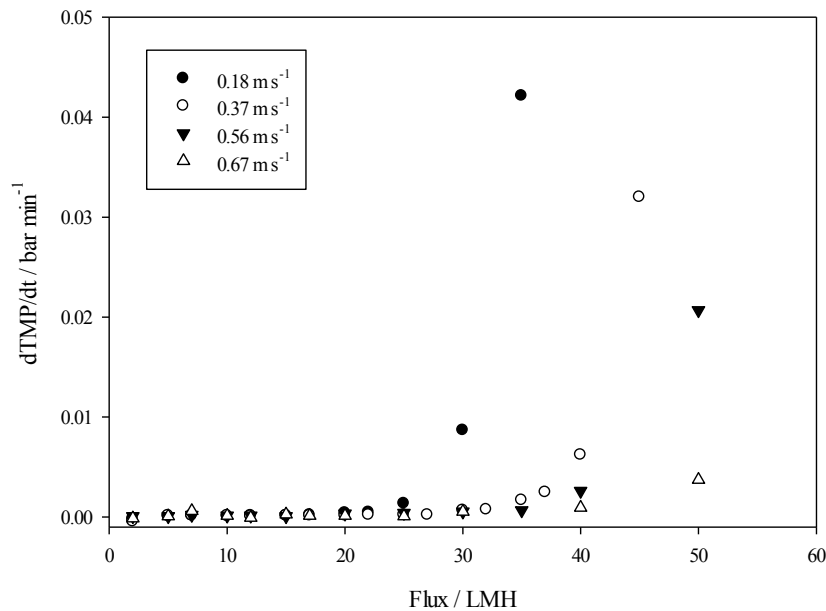


Figure 5: dTMP/dt for the filtration of 2wt% gum arabic with 0.1 μm PS membranes at different CFVs as a function of flux. The temperature was 40 °C

The critical fluxes can be determined from Figure 5 as 22, 32, 35 and 40 LMH for 0.18, 0.37, 0.56 and 0.67 ms^{-1} CFV, respectively and are shown graphically in Figure 6.

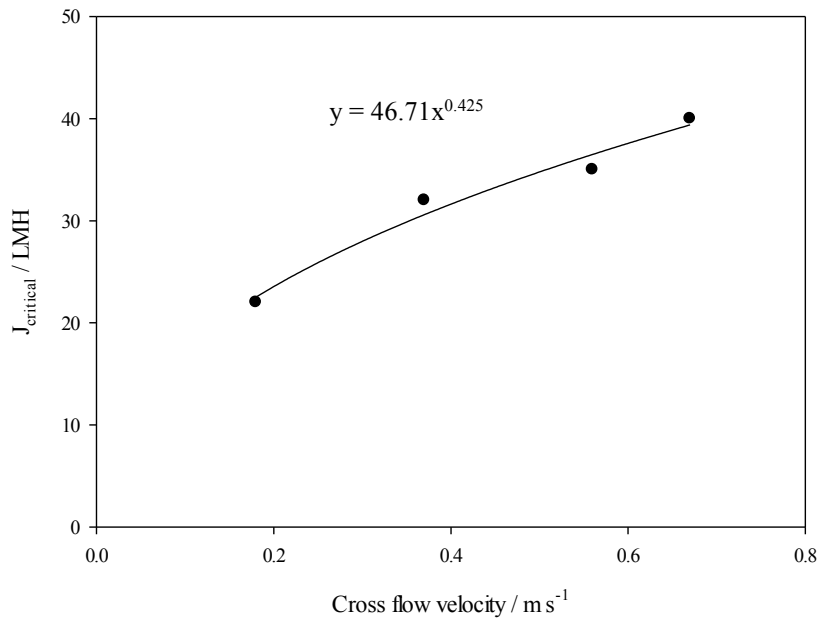


Figure 6: Critical flux values for 2 wt% gum arabic at 40 °C and varying CFVs with 0.1 μm PS membranes.

The relationship between flux and CFV can be described using the following equation:

$$J = f(V)^\alpha \quad (4)$$

The value of α varies depending on the system conditions but is typically between 0.3 – 1.33 for laminar flow, with the most common values lying between 0.3 and 0.6 (Cheryan, 1998). The α value for this system was found to be 0.425.

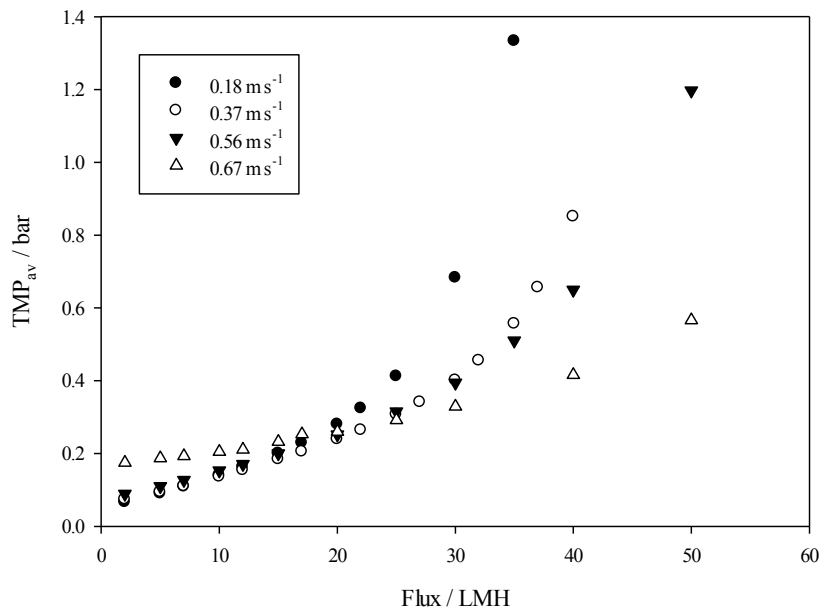


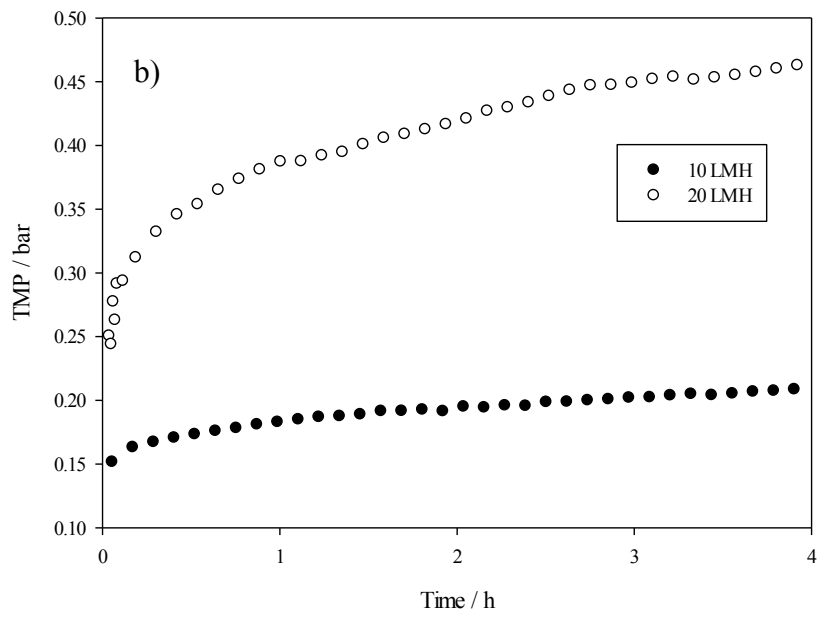
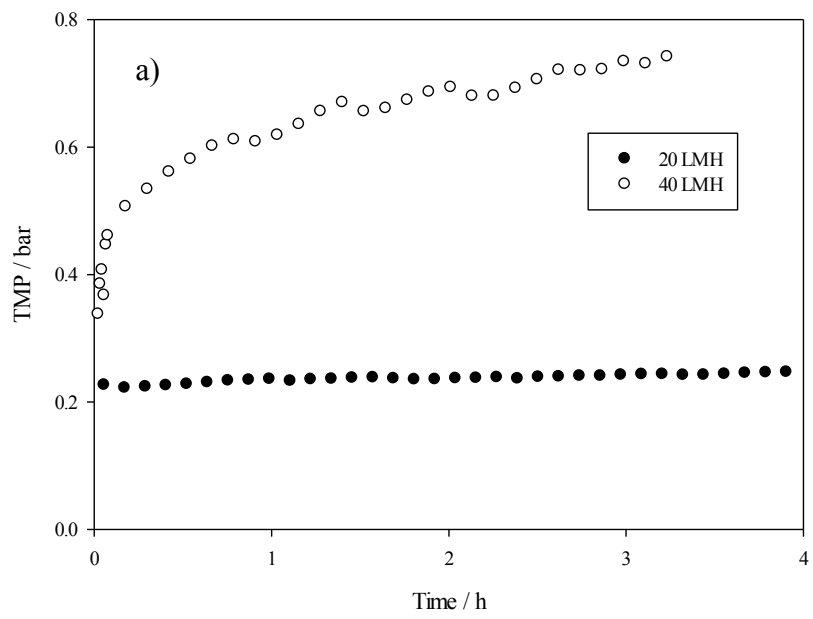
Figure 7: TMP_{av} for the filtration of 2wt% gum arabic with 0.1 μm PS membranes at different CFVs as a function of flux. The temperature was 40 °C

The critical fluxes determined from Figure 7 as the point at which K is no longer linear are 20, 27, 30 and 40 LMH for 0.18, 0.37, 0.56 and 0.67 ms^{-1} CFV, respectively.

The subcritical permeability constants for these 4 CFVs (85.5, 113.6, 93.4 and 161.2 $\text{L m}^{-2} \text{h}^{-1} \text{bar}^{-1}$, respectively) were observed to be lower than the corresponding constants for pure water (769.2, 625.0, 416.7 and 714.3 $\text{L m}^{-2} \text{h}^{-1} \text{bar}^{-1}$, respectively), indicating the weak form of the critical flux.

3.4. Fouling above and below the critical flux

Fouling experiments of 4 h duration were carried out in diafiltration mode with 2 wt% gum arabic above and below the critical fluxes determined above. Feed and permeate samples were collected and analysed for total solids, AGP and protein rejection.



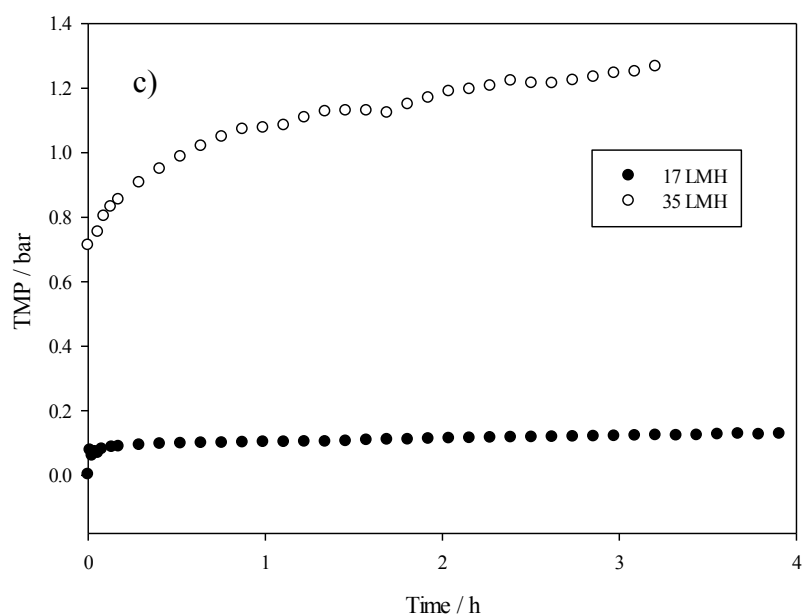


Figure 8: TMP fouling curves for the filtration of 2 wt% gum arabic using 0.1 μm (a), 0.5 μm (b) and 0.8 μm (c) PS membranes above and below the critical flux. Filtration temperature was 40 $^{\circ}\text{C}$ and the CFV was 0.37 m s^{-1}

Tables 1a and b shows the solids rejection and the protein and AGP content of the permeate from the filtration of 2 wt% gum arabic using 0.1, 0.5 and 0.8 μm PS membranes at fluxes above and below the determined critical flux. The protein mass fraction of the feed was 0.052 ± 0.01 and all protein values were calculated from elemental analysis by multiplying the %N by a conversion factor of 6.6 (Anderson, 1986). The feed AGP mass fraction was 0.187 ± 0.012 .

Table 1a: Solids rejection, protein mass fraction and AGP mass fraction of the permeate for filtration of 2 wt% gum arabic with 0.1, 0.5 and 0.8 μm PS below critical flux

| Membrane | Rejection | Permeate protein mass fraction | Permeate AGP mass fraction |
|-------------------|-----------|---------------------------------|---------------------------------|
| 0.1 μm | 0.99 | <i>Insufficient sample mass</i> | <i>Insufficient sample mass</i> |
| 0.5 μm | 0.96 | 0.083 | 0.087 |
| 0.8 μm | 0.6 | 0.035 | 0.133 |

Table 1b: Solids rejection, protein mass fraction and AGP mass fraction of the permeate for filtration of 2 wt% gum arabic with 0.1, 0.5 and 0.8 μm PS above critical flux.

| Membrane | Rejection | Permeate protein mass fraction | Permeate AGP mass fraction |
|-------------------|-----------|--------------------------------|----------------------------|
| 0.1 μm | 0.95 | 0.095 | 0.009 |
| 0.5 μm | 0.97 | 0.082 | 0.085 |
| 0.8 μm | 0.92 | 0.07 | 0.108 |

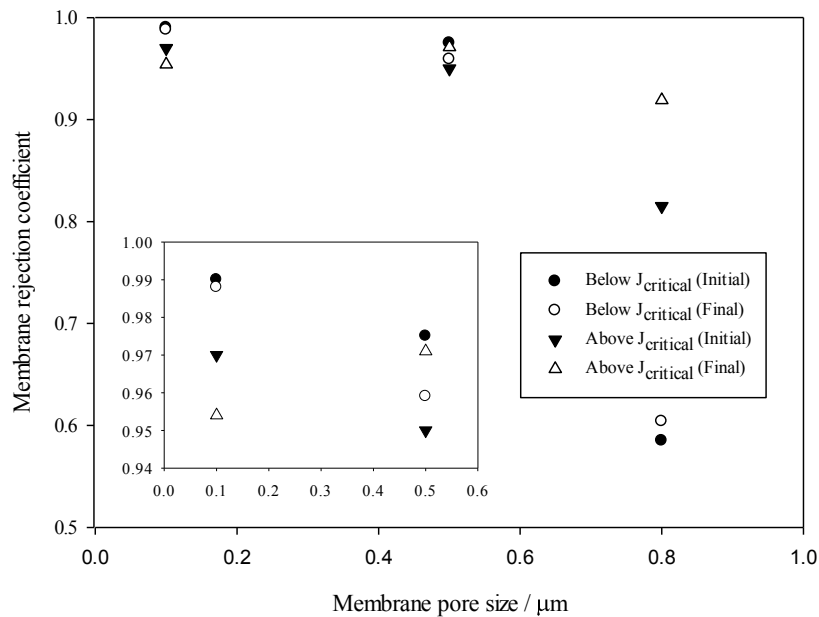


Figure 9: Rejection coefficients for the filtration of 2 wt% gum arabic using 0.1, 0.5 and 0.8 μm PS membranes above and below J_{critical} . Rejection coefficients are shown for the first 100 mL permeate (initial) and an average of the rest of the permeate (final).

4. DISCUSSION

4.1. Effect of membrane pore size

Membranes with a higher porosity should demonstrate an overall higher critical flux for the same feed under the same conditions due to a better distribution of the permeate flux across the membrane surface, minimising fouling build up in certain areas (Bacchin *et al.*, 2006). The pure water flux for the three pore sized membranes (virgin) increases proportionally with the pore size but it was shown in previous work that the total resistance when filtering 2 wt% gum was 5.8×10^{12} , 6.1×10^{12} and $3.3 \times 10^{12} \text{ m}^{-1}$ for 0.1, 0.5 and 0.8 μm PS membranes, respectively (Manning and Bird, 2015). This suggests that the 0.5 μm membrane fouls more readily than the other two membranes tested. This is perhaps due to a large proportion of the gum particles being of a similar size to the pores and the membrane being susceptible to pore plugging. It was concluded in this previous work that the 0.5 and 0.8 μm membranes were

fouled initially by pore blocking and then by formation of a cake layer on the surface. The pores of the 0.1 μm membrane were too small to allow much gum arabic into the internal structure (this was seen by $> 97\%$ solids rejection) and very little pore blocking occurred.

The values for critical flux observed here show that the 0.5 μm membrane had a lower critical flux than the 0.8 μm . This is likely to be due to the higher porosity in the larger pore sized membrane and the higher fouling propensity observed with the 0.5 μm membrane as discussed above. The 0.1 μm membrane demonstrated a higher critical flux than expected, based on the membrane pore size. This can be explained by a lack of pore blocking which occurs with the 0.5 and 0.8 μm membranes. Cake formation is the main fouling mechanism, which starts to be significant at higher fluxes than the pore blocking mechanism.

4.2. Effect of CFV

Increasing the CFV had the effect of increasing the critical flux value. The values determined by $d\text{TMP}/dt$ were 22 LMH, 32 LMH, 35 LMH and 40 LMH for 0.18, 0.37, 0.56 and 0.67 m s^{-1} , respectively.

These experiments into the effect of CFV upon the critical flux show that the flux at which fouling becomes significant increases quite considerably within the range studied. The largest increase occurs towards the lower end of the CFVs tested. The increase in CFV creates a greater shear across the surface of the membrane, reducing the boundary layer thickness. An increase in shear induced back diffusion also occurs, reducing the particle concentration at the membrane surface and minimising the risk of fouling at low permeate fluxes.

As the CFV is increased, however, a greater pressure drop across the membrane is seen and this results in a higher TMP at the inlet which may be super-critical, even if the average over the membrane is subcritical. This can result in increases in CFV having smaller effects on the critical flux increase at higher CFV values (Bacchin *et al.*, 2006). Table 2 shows the average pressure drop across the membrane for each of the experiments.

Table 2: The average pressure drops across a 0.1 μm PS membrane during the filtration of 2 wt% gum arabic at different CFVs

| Experiment cross flow velocity / m s^{-1} | Average pressure drop across the membrane / bar |
|--|---|
| 0.18 | 0.018 |
| 0.37 | 0.053 |
| 0.56 | 0.1 |
| 0.67 | 0.25 |

4.3. Fouling above and below critical flux

Figure 8 shows how TMP changes over time during the filtration of 2 wt% gum arabic above and below the critical flux measured above. For the 0.1 μm PS membrane, there is no TMP rise over 4 h of filtration at 20 LMH whereas at 40 LMH, a rapid initial increase is seen over

the first 30 minutes, followed by a more gradual yet still substantial increase after that. For the 0.5 μm membranes, (figure 14) a slight increase in TMP over time at 10 LMH shows that the critical flux in fact is a lower than previously thought. The curve at 20 LMH shows the same rapid increase in TMP flowed by a more gradual increase. This trend is also seen for the 0.8 μm membrane, with the flux of 17 LMH being sub-critical as no TMP rise is seen.

In all three fouling curves with operation above the critical flux, 2 distinct phases can be observed. The first is an initial, rapid rise in TMP due to concentration polarisation and the adsorption of species to the surface of the membrane causing pore closure / constriction. The second phase is a slower, steadier rise in TMP caused by the build-up of a cake layer (Ghosh, 2002). A higher super critical operation TMP is seen for the 0.8 μm membrane than for the other two membranes. This is likely to be due to the larger pore size of the membrane allowing for greater pore blocking as a larger proportion of the gum species are able to enter the pores. This is clear from the membrane rejection, which is lowest for the 0.8 μm membrane, but increases rapidly over time due to fouling (Figure 9).

From Tables 1a and b, it can be seen that both the 0.5 and 0.8 μm PS membranes display the expected trend of 0.5 μm permeate sample having lower solids content than the 0.8 μm permeate sample, due to the larger pore size of the 0.8 μm membrane allowing a greater proportion of the gum arabic to pass through. For the cases of filtration above the critical flux, the solids content drops from the first 100 mL permeate to the average over the whole filtration (between 400 – 600 mL permeate). This is because fouling of the internal membrane structure as well as cake formation on the surface effectively reduces the membrane pore size, reducing the amount of gum that can be transmitted by the membrane. In the case of the filtration below the critical flux, the solids content of the first 100 mL permeate is very similar to the average of the full permeate, which is because significant fouling of the membrane does not occur and so the filtration capability of the membrane is not affected.

The results from the 0.1 μm filtrations, however, are inconclusive. This is possibly due to the high error associated with the very small solids content of the permeate. Repeats of this experiment are required to obtain more reliable data.

Elemental analysis and GPC were carried out on permeate samples to determine the protein and AGP mass fractions (Tables 1a and b).

The protein and AGP mass fractions for the 0.5 μm membranes above and below the critical flux are almost identical. This is likely to be due to the ‘sub-critical’ experiment not in fact being below the critical flux as discussed above. Although the fouling was certainly more severe in the experiment at 20 LMH than the experiment at 10 LMH, this seems to have had little effect upon the fractionation. The permeate is depleted in AGP compared to the feed, however, showing that AGP is rejected by the membrane.

The 0.8 μm data show that a greater proportion of the AGP is rejected by the membrane at 35 LMH, above the critical flux. This is because the fouling enhances the fractionation performance of the membrane. However, the permeate still contains about 10 wt% AGP, so

this membrane alone is not sufficiently tight for effective gum arabic fractionation. Some feed or membrane modification is required to improve the AGP rejection.

The 0.1 μm membrane at super-critical flux shows almost complete rejection of AGP, which is very positive, however a high rejection of all gum solids is also seen, meaning the use of this membrane for fractionation would be very slow and both energy and water intensive.

Future work will investigate the use of more hydrophilic 0.5 and 0.8 μm membranes as well as modification of feed pH and ionic strength to improve the rejection of AGP.

5. CONCLUSION

The critical flux of 2 wt% gum arabic using 0.1, 0.5 and 0.8 μm PS membranes was determined to be 27, 12 and 22 LMH, respectively, at 40 °C and a CFV of 0.37 m s^{-1} . Experiments carried out at different CFV velocities showed the critical flux to increase with increasing CFV. Longer fouling tests were carried out above and below the determined critical flux and showed that the flux-stepping method is effective at estimating the critical flux over short (several hour) fouling runs. Analysis of the permeate shows that operating below the critical flux avoids membrane fouling and therefore, in the case of the 0.8 μm membrane, reduces the fractionation capability of the membrane. To further improve the fractionation of gum arabic using membranes, the use of other membrane materials and feed modification need to be investigated.

ACKNOWLEDGEMENTS

The authors would like to acknowledge Kerry Ingredients and Flavours for the supply of the gum arabic, Alfa Laval for the supply of the membranes and the EPSRC for funding through the Doctoral Training Centre at the University of Bath.

REFERENCES

- Al-Assaf, S., Phillips, G. O., Aoki, H. and Sasaki, Y. (2007) Characterization and properties of Acacia Senegal (L.) Willd. Var. Senegal with enhanced properties (Acacia (Sen) Super Gum (Tm)): Part 1 - Controlled maturation of Acacia Senegal Var. Senegal to increase viscoelasticity, produce a hydrogel form and convert a poor into a good emulsifier. *Food Hydrocolloids*, 21, 319-328.
- Anderson, D.M.W. (1986) Nitrogen conversion for the proteinaceous content of gums permitted as food-additives. *Food Additives and Contaminants*, 3, 231-234
- Bacchin, P., Aimar, P. and Field, R. W. (2006) Critical and sustainable fluxes: theory, experiments and applications. *Journal of Membrane Science*, 281, 42-69.
- Brans, G.; Schroën, C. G. P. H.; van der Sman, R. G. M.; Boom, R. M., (2004) Membrane fractionation of milk: state of the art and challenges. *Journal of Membrane Science*, 243, (1–2), 263-272.
- Cheryan, M. (1998) *Ultrafiltration and Microfiltration Handbook*, Boca Raton, USA, CRC Press.

- Chen, V., Fane, A. G., Madaeni, S. and Wenten, I. G. (1997) Particle deposition during membrane filtration of colloids: transition between concentration polarization and cake formation. *Journal of Membrane Science*, 125, 109-122.
- Fang, Y., Krulish, J. and Jendrysik, R. (2013) *Food and beverage emulsifiers*. US 08435581
- Field, R. W., Wu, D., Howell, J. A. and Gupta, B. B. 1995. Critical flux concept for microfiltration fouling. *Journal of Membrane Science*, 100, 259-272.
- Ghosh, R. (2002) Study of membrane fouling by BSA using pulsed injection technique. *Journal of Membrane Science*, 195, 115-123.
- Heidebach, T. and Sass, M. (2013) Preparing modified gum arabic useful in emulsion for beverage concentrate and ready-to-drink beverage involves treating gum arabic with an enzyme selected from glycosidases at specific concentration, EP2606750-A1.
- Katayama, T., Ido, T., Nishino, M., Inoue, T. and Phillips, G. O. (2012) Emulsification superiority of Super Gum™. *Gum Arabic*, The Royal Society Of Chemistry.
- Le Clech, P., Jefferson, B., Chang, I. S. and Judd, S. J. (2003) Critical flux determination by the flux-step method in a submerged membrane bioreactor. *Journal of Membrane Science*, 227, 81-93.
- Manning, H. E. and Bird, M. R. (2015) Gum arabic fractionation using synthetic membranes: the importance of fouling. *Food And Bioproducts Processing*, 93, 298-303.
- Nishino, M., Katayama, T., Sakata, M., Al-Assaf, S. and Phillips, G. O. (2012) Effect of AGP on emulsifying stability of gum arabic. *Gum Arabic*, The Royal Society Of Chemistry.
- Randall, R. C., Phillips, G. O. and Williams, P. A. (1988) The role of the proteinaceous component on the emulsifying properties of gum arabic. *Food Hydrocolloids*, 2, 131-140.
- Ward, F. M. (2002) Water-soluble esterified hydrocolloids. US 6455512.
- Weis, A., Bird, M. R., Nyström, M. and Wright, C. (2005) The influence of morphology, hydrophobicity and charge upon the long-term performance of ultrafiltration membranes fouled with spent sulphite liquor. *Desalination*, 175, 73-85.
- Ye, Y., Clech, P. L., Chen, V. & Fane, A. G. (2005) Evolution of fouling during crossflow filtration of model EPS solutions. *Journal of Membrane Science*, 264, 190-199.